Macromolecular Chemistry and Physics
www.mcp-journal.de

Liquid Metal–Ionic Liquid Composite Gels for Soft, Mixed Electronic–Ionic Conductors

*Juri Asada, Natsuka Usami, Hiroki Ota, Masayoshi Watanabe, and Kazuhide Ueno**

Mixed electronic–ionic conductors with high flexibility and stretchability can serve as key materials in rapidly emerging applications such as soft electronics and soft robotics. The combined use of two functional liquid materials, ionic liquids (ILs) and liquid metals (LMs), is of significant interest in the development of highly deformable mixed conductors. In this study, composite gels embedded with both IL and LM are prepared for the first time using a Ga–In eutectic (eGaIn), 1-ethyl-3-methyl imidazolium bis(trifluoromethanesulfonyl)amide, and poly(vinylidene fluoride-*co*-hexafluoropropylene) as the LM, IL, and polymer matrix, respectively. The composite gels exhibit low electronic conductivities of the order of 10^{-3} S cm^{-1}. The addition of an optimal amount of Ni particles (NiPs) improve the electronic conductivity to ≈25 S cm^{-1} while retaining mechanical flexibility. The electronic conductivity is further enhanced upon elongation due to the reversible alignment and elongation of the LM in the gel matrix along the stretching direction. Owing to a bicontinuous structure composed of the IL-based gel and metal component phases, the composite gels exhibit high ionic conductivity of the order of 10^{-3} S cm^{-1}. This study demonstrates a rational approach for designing stretchable mixed conductors using ILs and Ga-based LMs.

1. Introduction

Polymer gels, which are 3D polymer networks swollen by the presence of liquids, exhibit soft solid-like mechanical properties and liquid-like transport properties, and serve as crucial components in several applications.[1–3] Of particular importance in the field of electrochemical applications is gel electrolytes containing liquid electrolytes. These are employed in sensors and energy storage devices to suppress liquid electrolyte leakage and enhance the safety of electrochemical cells.[4–6] Extensive studies have been performed on gel electrolytes to achieve the mechanical properties of solid-state electrolytes while retaining the high ionic conductivity and mass transfer properties of liquid electrolytes.[7–9]

Gel electrolytes containing ionic liquids (ILs) in place of molecular liquid-based electrolytes, termed "ion gels," inherit many favorable properties from ILs, such as nonflammability, high ionic conductivity, and wide electrochemical potential windows.[10–12] IL-based gel electrolytes are promising as superior alternatives to conventional gel electrolytes for use in rechargeable batteries, fuel cells, solar cells, field-effect transistors, and polymer actuators.[13,14] Thus, the use of functional liquid materials as liquid components in polymer gels is a rational and beneficial strategy for developing soft functional materials.

Gallium-based liquid metals (LMs), such as Ga–In eutectic (Ga:In = 75.5:24.5 wt%; eGaIn) and Gallinstan (Ga:In:Sn = 66.5:20.5:13 wt%) have demonstrated significant potential for application in flexible and stretchable electronics[15–17] and soft robotics[18,19] owing to their high electronic (3.4×10^4 S cm^{-1})[20] and thermal (18.7 W m^{-1} K^{-1}) conductivities,[21] low viscosity (1.82 mPa s),[22] and low melting temperature (15.7 °C) (where the values correspond to eGaIn). In contrast to a typical LM such as Hg, Ga-based LMs are characterized by nonvolatility and low toxicity. Therefore, they are promising electron-conductive liquid materials, which can be useful in several applications under ambient conditions.[23,24] In an attempt to develop stretchable electric or thermal conductors capable of withstanding large deformations, polymer composites containing Ga-based LMs have been prepared using a range of polymeric materials, including silicone elastomers,[25,26] poly(styrene-isoprene-styrene) block copolymers,[27] polyurethanes,[28] polyacrylates,[29,30] and hydrogels[31,32] where the LMs are dispersed in the form of

J. Asada, N. Usami, K. Ueno
Department of Chemistry and Life Science
Yokohama National University
79-5 Tokiwadai, Hodogaya-ku, Yokohama 240-8501, Japan
E-mail: ueno-kazuhide-rc@ynu.ac.jp
H. Ota
Department of Mechanical Engineering
Yokohama National University
79-5 Tokiwadai, Hodogaya-ku, Yokohama 240-8501, Japan
M. Watanabe, K. Ueno
Advanced Chemical Energy Research Centre (ACERC)
Institute of Advanced Sciences
Yokohama National University
79-5 Tokiwadai, Hodogaya-ku, Yokohama 240-8501, Japan

The ORCID identification number(s) for the author(s) of this article can be found under https://doi.org/10.1002/macp.202100319

DOI: 10.1002/macp.202100319

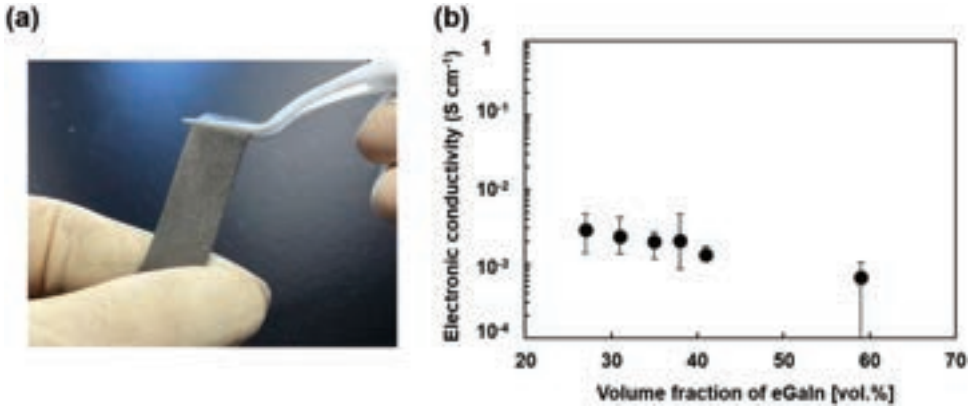

Figure 1. a) Photograph of the LM/IL composite gel containing 34 vol% of eGaIn. b) Electronic conductivity of the LM/IL composite gels with different eGaIn contents measured by the four-point probe method at room temperature.

droplets or infiltrated in the interconnected porous structure of the polymer matrices. Such polymer gels containing significant quantities of LMs may be termed as "metal gels" according to the scholarly classification based on the types of liquid components.

Highly deformable mixed conductors that enable the simultaneous conduction of electrons and ions play a pivotal role in stretchable electrochemical devices, such as wearable sensors[33] and stretchable batteries.[28,34] In this context, combinations of ILs and LMs are of significant interest for developing highly deformable mixed conductors owing to their unique properties, including high ionic/electronic conductivities, high thermal stability, negligible volatility, and high fluidity. However, polymer composite gels consisting of ILs and LMs have not been studied. In this paper, we report a composite gel comprising both an IL and a LM, using eGaIn, 1-ethyl-3-methyl imidazolium bis(trifluoromethanesulfonyl)amide ($[C_2mim][NTf_2]$), and poly(vinylidene fluoride-*co*-hexafluoropropylene) (PVDF-HFP) as the LM, IL, and polymer matrix, respectively. The incompatible eGaIn and $[C_2mim][NTf_2]$ were assembled into a bicontinuous structure of electronic and ionic conducting phases to endow mixed conducting properties. The electronic and ionic conductivities, and tensile properties were studied in the absence and presence of solid Ni particles (NiPs), and these properties were discussed in relation to the surface and internal structures of the composite gels.

2. Results and Discussions

2.1. LM/IL Composite Gels

Commercially available PVDF-HFP copolymers have been extensively studied as polymer matrices for gel electrolytes owing to their superior mechanical and electrochemical properties and facile gel preparation procedures.[8] A polymer gel swollen with an IL "ion gel" can be readily prepared using PVDF-HFP via the solution casting method.[35,36] The semicrystalline phases of the PVDF segments behave as physical crosslinking points, forming 3D polymer networks, whereas the well-developed amorphous domains of the copolymers containing the HFP moiety can accommodate large amounts of IL, which leads to a rubber-like solid form and high ionic conductivity of the order of 10^{-3} S cm^{-1}. For preparing the LM/IL-based mixed conductors, eGaIn was vigorously mixed with the pregel *N*-methyl-2-pyrrolidone (NMP) solution containing PVDF-HFP and $[C_2mim][NTf_2]$, and the mixture was then cast onto a perfluoroalkoxy alkane (PFA) Petri dish to form the LM/IL composite gels. This simple procedure allowed us to systematically prepare composite gel films with various eGaIn contents (up to 60 vol%) while maintaining the composition of the ion gel domain at PVDF-HFP/$[C_2mim][NTf_2]$ weight ratio of 3/7. However, the self-standing films were not formed with GaIn contents greater than 60%.

As shown in **Figure 1**a, the obtained gels were found to be uniformly gray, flexible, and self-standing without leakage of eGaIn, suggesting that the LM was dispersed throughout the composite gels without macroscopic phase separation and was securely embedded in the ion gel matrix. Figure 1b shows the electronic conductivity of the composite gels containing different eGaIn volume fractions measured using the four-point probe method. The parent LM, eGaIn, exhibits a high electronic conductivity of 3.4×10^4 S cm^{-1} in similarity with other metallic materials.[20] However, the electronic conductivities of the LM/IL composite gels drop significantly to the order of 10^{-3} S cm^{-1} across the range of eGaIn contents studied and the change in conductivity is marginal even with increasing proportion of the highly conductive LM. These results imply that the dispersed eGaIn provides a minor contribution to the electron conduction in the composite gels even at a LM content of 60 vol%, which is significant enough to exceed the percolation threshold[37] and is comparable to the random close packing density of spheres.[38]

To investigate the significantly low electronic conductivities of the composite gels, the cross-sectional and surface morphology of the composite gel with 34 vol% eGaIn was studied using scanning electron microscopy (SEM)-energy dispersive X-ray spectroscopy (EDX) analysis. As shown in the cross-sectional SEM image (**Figure 2**a) and the corresponding EDX mapping image (Figure 2b), eGaIn and the ion gel were segregated into two interpenetrating phases of the order of tens of micrometers. This proved that eGaIn was uniformly distributed and encapsulated in the composite gel, where the ion gel phase prevented macroscopic coalescence of the LM droplets. Although the SEM image shows that surface morphology is relatively smooth (Figure 2c), the corresponding EDX mapping image (Figure 2d)

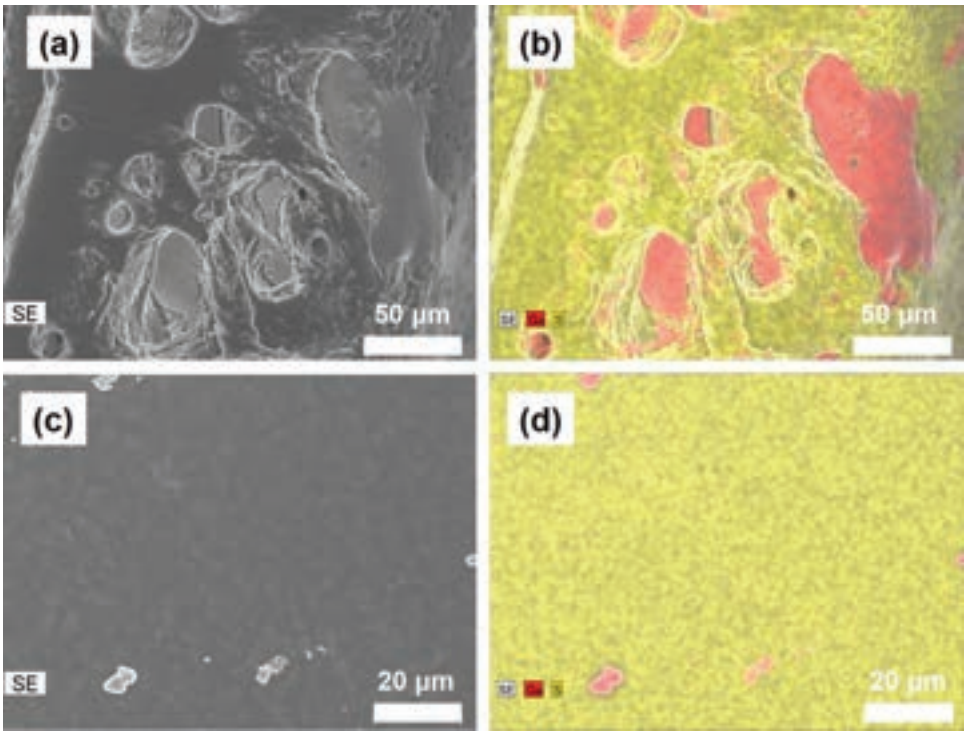

Figure 2. Cross-sectional a) SEM and b) EDX mapping images, and surface c) SEM and d) EDX mapping images of the LM/IL composite gel with 34 vol% eGaIn; red and yellow parts in the EDX images represent Ga and S elements, respectively.

clearly indicates that the ion gel component (represented as the S element of the $[NTf_2]$ anion, yellow) preferentially resides on the surface, and the LM component (represented as the Ga element, red) is hardly detected at the surface of the composite gel.

The surface tension of eGaIn (445 mN m^{-1})[22] is more than one order of magnitude higher than that of $[C_2mim][NTf_2]$ (35 mN m^{-1})[39] and PVDF-HFP (25 mN m^{-1}).[40] The LMs with inherently high surface energies[41] exhibit a lower affinity to the surface (i.e., air for the top and the PFA substrate for the bottom of the composite gel film) than the PVDF-HFP/$[C_2mim][NTf_2]$ ion gel. Therefore, eGaIn flows farther from the surface during gel preparation, and the surface component is dominated by the ion gel. The absence of the LM component at the surface is considered to be responsible for the significantly low electronic conductivity of the composite gels: the electron-insulating ion gel-rich surface blocks electron flow between the probe electrodes and composite gels. Ga-based LMs are known to easily develop a few-nm-thick oxide layer on the surface when exposed to air.[42] The insulating surface oxide layer of the dispersed eGaIn also contributes to the high contact resistance between the LM droplets, which leads to low conductivity.

2.2. LM/Ni/IL Composite Gels

The high fluidity of Ga-based LMs can be controlled by the addition of solid fillers.[43] The incorporation of a sufficient amount (2–10 wt%) of nano- or microsized NiPs in the LM modifies the rheological properties from liquid-like to soft solid (paste)-like.[44] To reduce the fluidity of eGaIn during the solvent casting process for gel preparation, microsized NiPs were added to the pregel solution as a conducting solid filler, and the LM/Ni/IL composite gels were prepared in the presence of NiPs. **Figure 3** presents the electronic conductivity of the LM/Ni/IL composite gels measured by the four-point probe method. The volume fraction of the total metal component (eGaIn and NiPs) in the composite gels was adjusted to a constant of 34 vol%, while the volume ratio of NiPs in the total metal component was varied (Figure 3a). The partial replacement of eGaIn with NiPs enhanced the electronic conductivity by four orders of magnitude. Furthermore, the LM/Ni/IL composite gels exhibited higher conductivities than composite gels containing solely NiPs as the metallic component (4.1 S cm^{-1}), and the conductivities reached a maximum value of ≈24 S cm^{-1} at a NiP volume ratio of 0.5 with respect to the total metal component. These results demonstrated that the coexistence of eGaIn and NiPs significantly enhanced the electronic conductivity of the composite gels.

In Figure 3b, the volume fraction of the total metal component (eGaIn and NiPs) was varied in the range of 12–45 vol%, whereas the volume ratio of NiPs in the metal component was adjusted to a constant value of 0.5. The electronic conductivity increased from 1.5 to 25 S cm^{-1} with increasing metallic content, but the value leveled off at 45 vol% of metal components. The electronic conductivity of the composite gel was significantly lower than the intrinsic values of the metallic materials (3.4×10^4 S cm^{-1} for eGaIn and 1.4×10^5 S cm^{-1} for Ni). It is postulated that the ion gel domain and the thin oxide layer formed on the eGaIn droplets[45,46] and NiPs partially obstructed the electron-conducting pathway, resulting in a high contact resistance between the dispersed metal components. However, the electronic

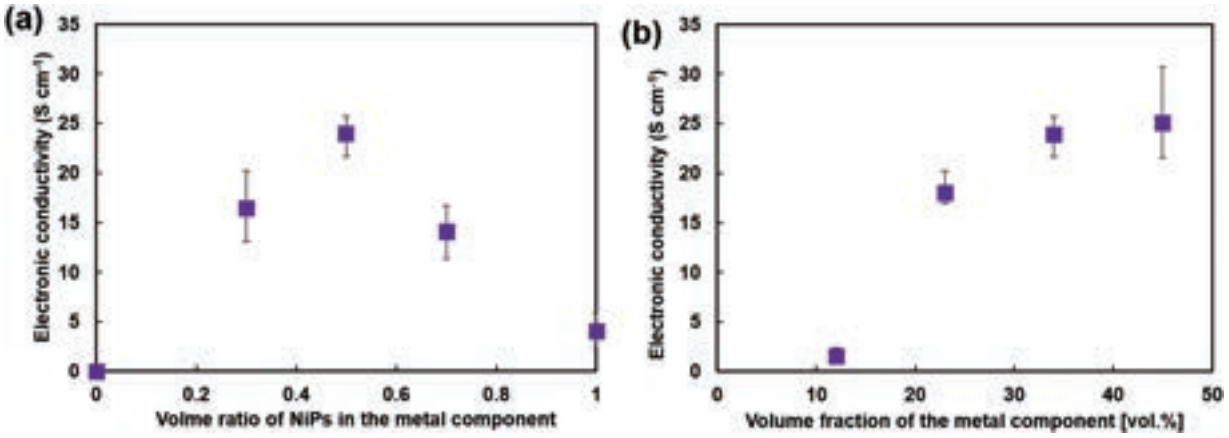

Figure 3. Conductivity of the LM/Ni/IL composite gels a) with the total metal component of 34 vol% and different volume ratios of NiPs in the metal component, and b) with different volume fractions of the metal component at a constant NiP volume ratio of 0.5.

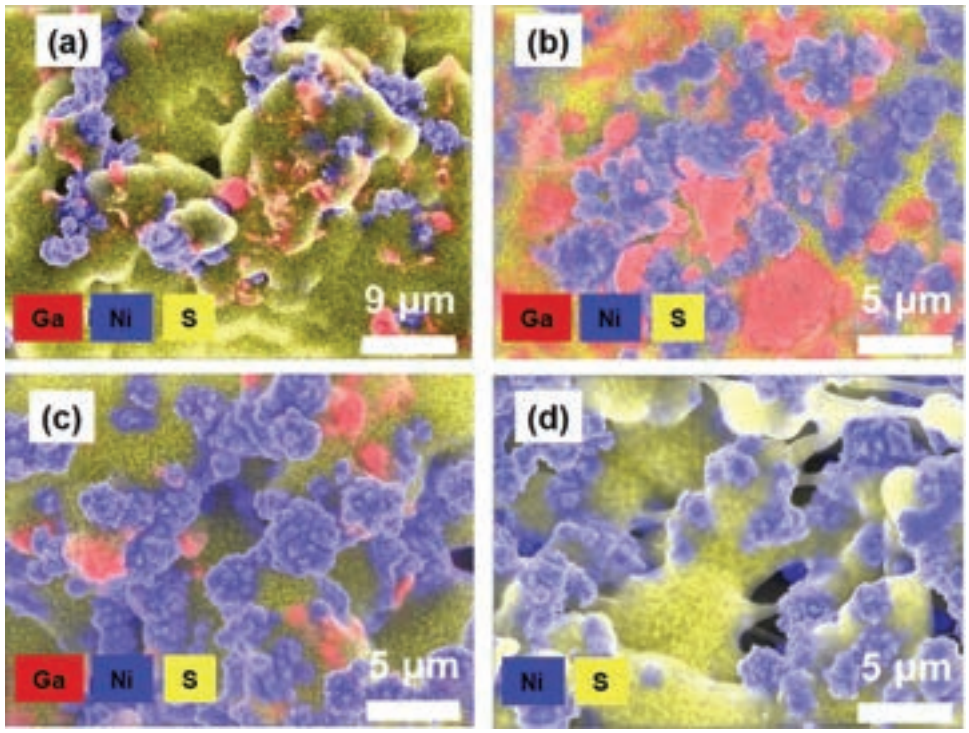

Figure 4. Surface EDX mapping images of the LM/Ni/IL composite gels with the total metal component of 34 vol% and different NiP volume ratios: a) 0.33, b) 0.5, c) 0.66, and d) 1; the red, blue, and yellow parts in the EDX images represent Ga, Ni, and S elements, respectively.

conductivity of the LM/Ni/IL composite gels was found to be adjustable in the range of 1.5–25 S cm^{-1} depending upon the metallic filler content and the proportion of eGaIn to NiP. High electronic conductivities exceeding 10^3 S cm^{-1} are reported for polymer composites with nonspherical fillers such as metallic nanowires,[47] nanosheets,[48] and nanoplatelets,[49,50] which allow more efficient percolation of the conduction pathway. In addition, the type of the metallic fillers is known to affect the electronic conductivity of polymer composites.[51] Likewise, the use of highly conductive solid fillers with higher aspect ratios can further enhances the electronic conductivity of the composite gels.

Figure 4 displays the surface morphologies of the LM/Ni/IL composite gels with 34 vol% total metal components and different NiP volume ratios. The EDX mapping images of the LM/Ni/IL composite gels (Figure 4a–c) indicate that the metal components (both eGaIn and NiPs) reside on the surface of the composite gels, unlike the LM/IL composite gels (Figure 2d). The addition of NiPs reduces the mobility of eGaIn during gel preparation, and the ion gel domain and NiPs successfully immobilize the LM component on the surface. The LM droplets and NiPs come in direct contact, presumably because of the high affinity between these metallic materials,[43] and form an

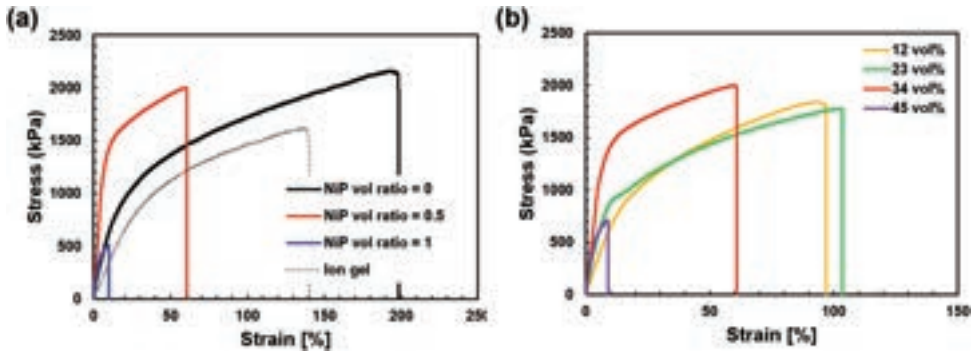

Figure 5. Stress–strain curves of the LM/Ni/IL composite gels with a) the total metal component of 34 vol% and different volume ratios of NiPs in the metal component, and b) different volume fractions of the metal component at a constant NiP volume ratio of 0.5.

electron-conducting network that leads to the enhanced conductivity of the LM/Ni/IL composite gels. In the LM/Ni/IL composite gels with a lower volume ratio of NiPs (Figure 4a), lower proportions of surface metal components (eGaIn and NiPs) are observed, and the ion gel domain accounts for a significant portion. Larger amounts of eGaIn and NiPs are observed at a NiP volume ratio of 0.5 (Figure 4b), and the interconnected NiP aggregates are efficiently linked by the dispersed eGaIn phases. This corroborates the maximum conductivity at a NiP volume ratio of 0.5 (Figure 3a). The amount of eGaIn at the surface appears to be lesser in association with the lower LM content at a higher NiP volume ratio (Figure 4c). In contrast to the LM/Ni/IL composite gels, there were larger numbers of pores in the composite gels fabricated solely with NiPs (Figure 4d). It is thus feasible that the lower conductivity of the composite gel with NiPs as compared to that of the LM/Ni/IL composite gels is due to the large number of insulating pores.

Tensile tests were performed to study the mechanical properties of the LM/Ni/IL composite gels, and the stress–strain curves are shown in **Figure 5**. Figure 5a depicts the tensile properties of the composite gels with a total metal component of 34 vol%. The LM/IL composite gel without the NiPs (NiP volume ratio of 0) exhibited remarkable deformation properties with a fracture strain of 195% and a tensile strength of 2.1 MPa at break. These values are larger than those of the parent ion gel: fracture strain of 140% and a tensile strength of 1.6 MPa. Hence, the LM had a non-negligible impact on the mechanical properties, and the composite gel was stiffened in presence of 34 vol% LM. On the basis of an extended Eshelby's theory considering the surface tension of the solid–liquid interface, the counter-intuitive reinforcement of mechanical properties was reported theoretically[52] and experimentally[53,54] for soft solids embedded with liquid droplets such as Ga-based LMs. The deformability and dynamic rearrangement of the LM droplets was also found to be responsible for effective energy dissipation, adaptive crack movement, and elimination of the crack tip, leading to the toughening of the soft materials.[25]

In contrast, the addition of solid NiPs impairs the mechanical properties. The composite gel containing solely NiPs (NiP volume ratio of 1) exhibited a significantly lower fracture strain of 10% and tensile strength of 0.5 MPa, indicating that the composite gels became more brittle and significantly less flexible and stretchable in the presence of the solid NiP fillers. The LM/Ni/IL composite gel with a NiP volume ratio of 0.5 demonstrated intermediate mechanical properties. Compared with the LM/IL composite gels without NiPs, the decrease in the tensile strength observed upon combining the LM and solid filler was insignificant (2 MPa). However, the fracture strain decreased to 61%. These results encouraged further studies on the mechanical properties. An optimized composition of eGaIn and NiPs can potentially retain the highly deformable properties of the composite gels in addition to the enhancement of electronic conductivity.

Figure 5b shows the stress–strain curves of the LM/Ni/IL composite gels with different volume fractions of the total metal components in which the NiP volume ratio is 0.5. Composite gels with metal component proportions lower than 23 vol% can mitigate the decrease in the fracture strain to ≈100% while retaining a tensile strength of ≈2.0 MPa. However, further increase in the metal component to 45 vol% was found to drastically reduce both the fracture strain (10%) and tensile strength (0.7 MPa). A total proportion of metal component in the range of 23–34 vol% and NiP volume ratio of 0.5 was the optimum composition for the LM/Ni/IL composite gels in terms of the electronic conductivity (Figure 3) and the mechanical properties (Figure 5).

The electronic conductivities of the LM/Ni/IL composite gels were further investigated under the effects of stretching. As shown in **Figure 6**a, for the composite gel containing 34 vol% rigid NiPs, the electronic conductivity ratio σ/σ_0 decreases to 60% prior to rupture at 5% strain. The pristine interconnections of the NiP aggregates gradually loosen upon stretching, which breaks the electrical pathway in the composite gels. Such behavior is typical of conductive polymer composites using solid fillers. Most of the stretchable conductors were reported to exhibit continuous decay of electronic conductivity upon elongation owing to a similar mechanism.[55] In contrast, the LM/Ni/IL composite gel with 23 vol% metal components exhibited a linear increase in σ/σ_0 with increase in the elongation strain, and σ/σ_0 reached ≈250% at the breaking point (Figure 6b). Clearly, eGaIn played an essential role in this atypical enhancement of electronic conductivity upon elongation. A similar stretch-induced enhancement in conductivity is reported for a macroporous silicone elastomer embedded with a 3D Ga-based LM network.[26] Micro-X-ray tomography and mechanoelectrical modeling revealed that the Ga-based LM elongates to align with the stretching and electric field directions, offering a more straightforward conduction route compared to the significantly

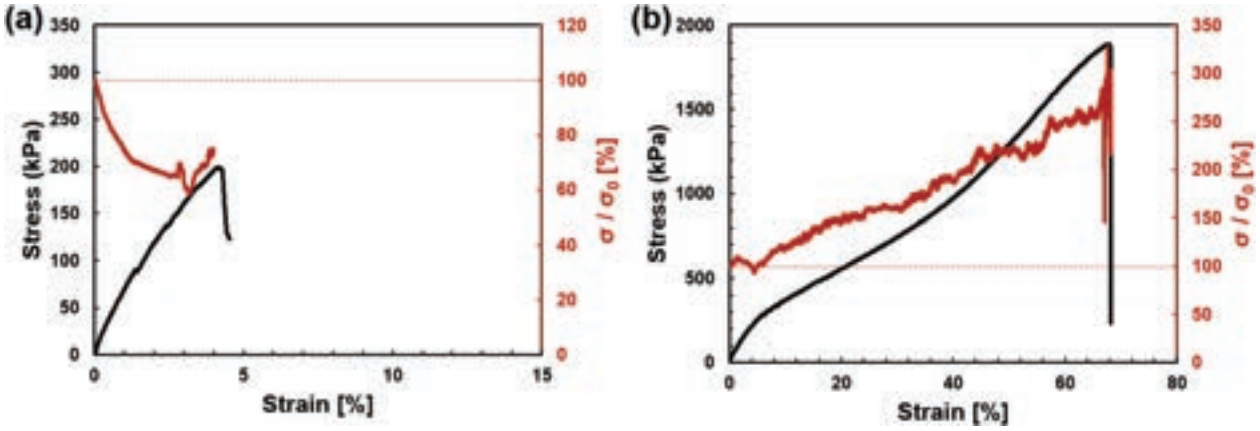

Figure 6. Stress–strain curves and the strain-dependent conductivity ratio σ/σ_0 of a) the composite gels with 34 vol% of NiPs and b) the LM/Ni/IL composite gel with 23 vol% metal components and NiP volume ratio of 0.5.

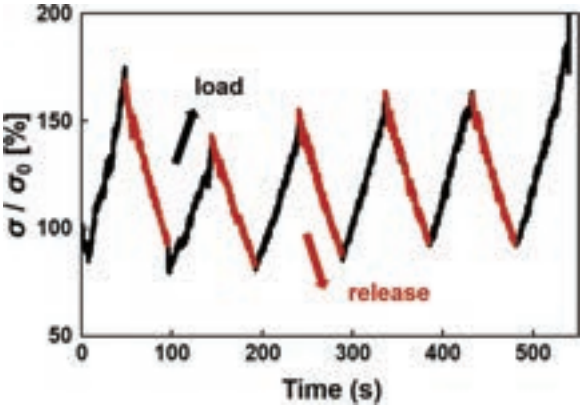

Figure 7. The change in σ/σ_0 of the LM/Ni/IL composite gel with 23 vol% metal components and NiP volume ratio of 0.5 in the load–release cycles with 30% elongation strain.

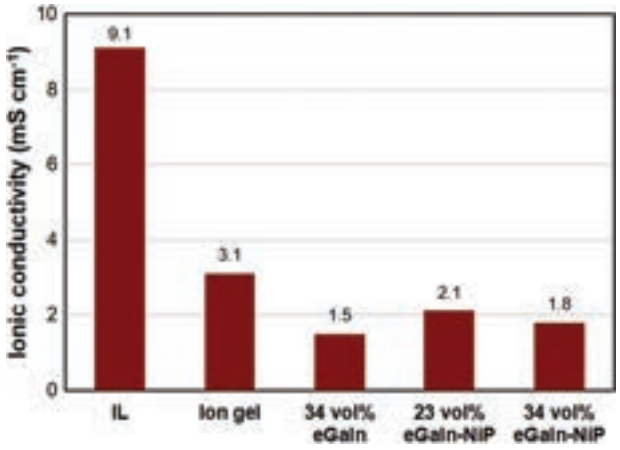

Figure 8. Ionic conductivity of the IL, $[C_2mim][NTf_2]$, ion gel, and composite gels at 25 °C. The LM/Ni/IL composite gels contained 23 or 34 vol% metal components while the NiP volume ratio was fixed at 0.5. The LM/IL composite gels contained 34 vol% eGaIn. The ionic conductivity of $[C_2mim][NTf_2]$ was obtained from ref. [56].

tortuous route of the original state. Similarly, the stretch-induced alignment and elongation of the freely deformable eGaIn connects the NiP aggregates more effectively with the electric field, resulting in the enhanced conductivity of the LM/Ni/IL composite gels upon elongation. As shown in **Figure 7**, the change in σ/σ_0 was monitored in the load–release cycles with 30% elongation strain. It was observed that σ/σ_0 increased monotonically upon stretching, but recovered to almost 100% when the applied load was released. Moreover, the change in σ/σ_0 was nearly reversible in repeated cycles. These results suggest that eGaIn embedded in the rubber-like ion gel matrix enables a reversible change in the internal structure during load–release cycles.

As shown in Figure 4, the LM/Ni/IL composite gels form a bicontinuous phase comprising the ion gel and metallic components (eGaIn and NiPs) and are proposed as a flexible and stretchable mixed electronic–ionic conductor. **Figure 8** depicts the ionic conductivity measured by the complex impedance method with the aid of a three-layered (ion gel/composite gel/ion gel) structure, where the ion gel layers are responsible for the electron-blocking. Due to experimental difficulty of the impedance measurement upon stretching, ionic conductivity of the composite gels was studied without strain. Despite the presence of 70 wt% IL, the ion gel exhibits an ionic conductivity of 3.1 mS cm^{-1} at 25 °C, which is 34% of that exhibited by neat $[C_2mim][NTf_2]$ (9.1 mS cm^{-1}). The decrease in ionic conductivity is due to the lowered mobility of the ions solvated in the amorphous phase and increased tortuosity in the semicrystalline PVDF-HFP network. Ionic conduction is further impeded in the presence of eGaIn and NiPs, leading to a further decrease in the ionic conductivity in the composite gels. The ionic conductivity obtained for the LM/IL composite gel with 34 vol% eGaIn was 1.5 mS cm^{-1}. As expected, the lower content of eGaIn and NiPs results in higher ionic conductivity: 2.1 and 1.8 mS cm^{-1} for the LM/Ni/IL composite gels with 23 and 34 vol% metallic components, respectively, which are slightly higher than that of the LM/IL composite gels. As a result, the composite gels show relatively high ionic conductivities of the order of 10^{-3} S cm^{-1} at 25 °C.

3. Conclusion

We have successfully prepared LM/IL composite gels by combining eGaIn and [C_2mim][NTf_2] with PVDF-HFP using a facile solvent casting method. The LM/IL composite gels exhibited tensile properties comparable to those of the parent ion gel without eGaIn leakage. However, the electronic conductivity was significantly low ($\approx 10^{-3}$ S cm^{-1}), predominantly due to the absence of LM at the outermost surface of the LM/IL composite gels. The addition of NiPs modified the surface morphology, resulting in the formation of eGaIn–NiP-enriched surface, which improved the electronic conductivity to $\approx$25 S cm^{-1}. Although the composite gels were stiffer and less stretchable in presence of the rigid NiP fillers, optimized proportions of eGaIn and NiPs enabled highly deformable properties without compromising electronic conductivity. In contrast to typical stretchable conductors with solid fillers, the electronic conductivity of the LM/Ni/IL composite gels increased monotonically increased upon elongation until the breaking point. The alignment and elongation of the LM along the direction of elongation imparted a primarily rectilinear conduction path, resulting in the stretch-induced enhancement of the electronic conductivity. In addition to electronic conduction, the LM/Ni/IL composite gels exhibited ionic conductivity values of the order of 10^{-3} S cm^{-1} owing to the bicontinuous internal structure consisting of the ion gel and metal component phases. The LM/Ni/IL composite gels prepared from thermally stable and negligibly volatile IL and LM are promising electronic–ionic conductors for stretchable devices such as wearable sensors and electroactive polymer actuators. However, the electronic conductivity and mechanical properties require further improvement to enable the use of such composite gels in stretchable electrode materials for energy storages and integrated electronic circuits that demand high and stable electronic conductivity under strain. Further optimization of metallic solid fillers and polymer matrices would achieve higher conductivity and stretchability of LM/IL composite gels.

4. Experimental Section

eGaIn (Ga:In = 75.5:24.5 wt%) and Ni powder (NiP, <50 μm) were purchased from Sigma-Aldrich and used as received without further purification. PVDF-HFP (Kynar flex 2801) was provided by Arkema and used as received. An IL, [C_2mim][NTf_2], was synthesized and purified according to a previously reported procedure.[56] NMP was obtained from FUJIFILM Wako Chemicals. PVDF-HFP and [C_2mim][NTf_2] were dissolved in NMP at a weight ratio of PVDF-HFP:[C_2mim][NTf_2] = 3:7, and eGaIn and/or NiPs were added to the composite gel solution at a given volume ratio to prepare a slurry. The slurry was subjected to vigorous mechanical mixing for 15 min using a conditioning mixer (AR-250, THINKY) to ensure homogeneous dispersion, which was followed by degassing for 30 s to remove air bubbles. The slurry was then poured into a PFA Petri dish, and NMP solvent was allowed to evaporate in an oven at 80 °C for 12 h. The composite gel membranes were peeled off from the Petri dish and further dried in vacuum at 80 °C for 12 h. The typical thickness of the prepared membranes was 400–600 μm. The ion gels were prepared using a procedure similar to the composite gels without the metal components.

The composite gels were cut into 12 mm disks, and subjected to electronic and ionic conductivity measurements. The electronic conductivity was measured using a four-point probe resistivity meter (MCP-T610, Mitsubishi Chemical Analytech) equipped with a PSP probe at room temperature. A 12 mm circular-shaped, three-layered gel (ion gel/composite gel/ion gel) was prepared for ionic conductivity measurements, in which the ion gel layers allowed ionic contact while eliminating electrical contact between the composite gel and the electrode. The three-layered gel was placed between two polished stainless-steel disk electrodes in an airtight two-electrode cell. The total ionic resistance of the three-layered gel was determined using the complex impedance method with a Hewlett-Packard 4192A impedance analyzer in the frequency range of 13 MHz to 5 Hz at an oscillation amplitude of 10 mV. For ionic conductivity measurement, the cells were thermally equilibrated at 25 °C for 1 h using an SU-261 constant temperature oven (ESPEC, Japan). The ionic resistance of the composite gels was obtained by subtracting the ionic resistance of the two ion gel layers from the overall ionic resistance of the three-layered gel, followed by conversion to the effective ionic conductivity of the composite gel.

The gel samples were cut into dumbbell shapes for the tensile tests. The tensile properties were analyzed using a Shimadzu EZ-LX instrument at a crosshead speed of 5 mm min^{-1}. The change in the electronic conductivity upon uniaxial elongation was studied using the tensile tester equipped with a potentio/galvanostat (ALS Model701Ex). A constant voltage of 50 mV was applied between the chucks along the direction of the elongation, and the DC current was simultaneously recorded during the tensile test. The resistivity of the composite gels was converted to the electronic conductivity by assuming a Poisson's ratio of 0.5 since Poisson's ratio of rubbery materials and gels are known to be nearly 0.5.[57,58] The morphologies of the composite electrolytes were observed using field-emission scanning electron microscopy (FE-SEM, SU8010, Hitachi). EDX was performed in conjunction with SEM.

Acknowledgements

This research was supported in part by JSPS KAKENHI (Grant Nos. 19K22216 to K.U. and 20H00213 to H.O.) and JST CREST (Grant Number JPMJCR1905), Japan.

Conflict of Interest

The authors declare no conflict of interest.

Data Availability Statement

The data that support the findings of this study are available from the corresponding author upon reasonable request.

Keywords

composite gels, Ga–In eutectic, ionic liquids, liquid metals, mixed electronic–ionic conductors

Received: August 27, 2021
Revised: October 28, 2021
Published online:

[1] Y. Osada, J. Ping Gong, Y. Tanaka, *J. Macromol. Sci., Part C: Polym. Rev.* **2004**, *44*, 87.
[2] M. Shibayama, *Soft Matter* **2012**, *8*, 8030.
[3] P. Zarrintaj, M. Jouyandeh, M. R. Ganjali, B. S. Hadavand, M. Mozafari, S. S. Sheiko, M. Vatankhah-Varnoosfaderani, T. J. Gutiérrez, M. R. Saeb, *Eur. Polym. J.* **2019**, *117*, 402.
[4] M. Armand, *Solid State Ionics* **1983**, *9–10*, 745.
[5] W. Glasspool, J. Atkinson, *Sens. Actuators, B* **1998**, *48*, 308.

[6] A. K. Arof, I. M. Noor, M. H. Buraidah, T. M. W. J. Bandara, M. A. Careem, I. Albinsson, B.-E. Mellander, *Electrochim. Acta* **2017**, *251*, 223.
[7] J. Y. Song, Y. Y. Wang, C. C. Wan, *J. Power Sources* **1999**, *77*, 183.
[8] M. Zhu, J. Wu, Y. Wang, M. Song, L. Long, S. H. Siyal, X. Yang, G. Sui, *J. Energy Chem.* **2019**, *37*, 126.
[9] X. Cheng, J. Pan, Y. Zhao, M. Liao, H. Peng, *Adv. Energy Mater.* **2018**, *8*, 1702184.
[10] M. A. B. H. Susan, T. Kaneko, A. Noda, M. Watanabe, *J. Am. Chem. Soc.* **2005**, *127*, 4976.
[11] T. P. Lodge, T. Ueki, *Acc. Chem. Res.* **2016**, *49*, 2107.
[12] M. Forsyth, L. Porcarelli, X. Wang, N. Goujon, D. Mecerreyes, *Acc. Chem. Res.* **2019**, *52*, 686.
[13] D. R. Macfarlane, M. Forsyth, P. C. Howlett, M. Kar, S. Passerini, J. M. Pringle, H. Ohno, M. Watanabe, F. Yan, W. Zheng, S. Zhang, J. Zhang, *Nat. Rev. Mater.* **2016**, *1*, 15005.
[14] M. Watanabe, M. L. Thomas, S. Zhang, K. Ueno, T. Yasuda, K. Dokko, *Chem. Rev.* **2017**, *117*, 7190.
[15] P. Won, S. Jeong, C. Majidi, S. H. Ko, *iScience* **2021**, *24*, 102698.
[16] T. Kozaki, S. Saito, Y. Otsuki, R. Matsuda, Y. Isoda, T. Endo, F. Nakamura, T. Araki, T. Furukawa, S. Maruo, M. Watanabe, K. Ueno, H. Ota, *Adv. Electron. Mater.* **2020**, *6*, 1901135.
[17] N. Ochirkhuyag, R. Matsuda, Z. Song, F. Nakamura, T. Endo, H. Ota, *Nanoscale* **2021**, *13*, 2113.
[18] R. Guo, H. Wang, M. Duan, W. Yu, X. Wang, J. Liu, *Smart Mater. Struct.* **2018**, *27*, 085022.
[19] K. Matsubara, D. Tachibana, R. Matsuda, H. Onoe, O. Fuchiwaki, H. Ota, *Adv. Intell. Syst.* **2020**, *2*, 2000008.
[20] Y. Gao, H. Li, J. Liu, *PLoS One* **2013**, *8*, e69761.
[21] Y.-G. Park, H. Min, H. Kim, A. Zhexembekova, C. Y. Lee, J.-U. Park, *Nano Lett.* **2019**, *19*, 4866.
[22] Q. Xu, N. Oudalov, Q. Guo, H. M. Jaeger, E. Brown, *Phys. Fluids* **2012**, *24*, 063101.
[23] M. D. Dickey, *ACS Appl. Mater. Interfaces* **2014**, *6*, 18369.
[24] X. Sun, B. Yuan, W. Rao, J. Liu, *Biomaterials* **2017**, *146*, 156.
[25] N. Kazem, M. D. Bartlett, C. Majidi, *Adv. Mater.* **2018**, *30*, 1706594.
[26] B. Yao, W. Hong, T. Chen, Z. Han, X. Xu, R. Hu, J. Hao, C. Li, H. Li, S. E. Perini, M. T. Lanagan, S. Zhang, Q. Wang, H. Wang, *Adv. Mater.* **2020**, *32*, 1907499.
[27] R. Tutika, A. B. M. T. Haque, M. D. Bartlett, *Commun. Mater.* **2021**, *2*, 64.
[28] S. Park, G. Thangavel, K. Parida, S. Li, P. S. Lee, *Adv. Mater.* **2019**, *31*, 1805536.
[29] J. Yan, M. H. Malakooti, Z. Lu, Z. Wang, N. Kazem, C. Pan, M. R. Bockstaller, C. Majidi, K. Matyjaszewski, *Nat. Nanotechnol.* **2019**, *14*, 684.
[30] C. J. Thrasher, Z. J. Farrell, N. J. Morris, C. L. Willey, C. E. Tabor, *Adv. Mater.* **2019**, *31*, 1903864.
[31] J.-E. Park, H. S. Kang, J. Baek, T. H. Park, S. Oh, H. Lee, M. Koo, C. Park, *ACS Nano* **2019**, *13*, 9122.
[32] C. Xu, B. Ma, S. Yuan, C. Zhao, H. Liu, *Adv. Electron. Mater.* **2020**, *6*, 1900721.
[33] Y.-G. Park, G.-Y. Lee, J. Jang, S. M. Yun, E. Kim, J.-U. Park, *Adv. Healthcare Mater.* **2021**, *10*, 2002280.
[34] D. G. Mackanic, M. Kao, Z. Bao, *Adv. Energy Mater.* **2020**, *10*, 2001424.
[35] S. K. Hwang, T. J. Park, K. L. Kim, S. M. Cho, B. J. Jeong, C. Park, *ACS Appl. Mater. Interfaces* **2014**, *6*, 20179.
[36] G. P. Pandey, S. A. Hashmi, *Electrochim. Acta* **2013**, *105*, 333.
[37] T. Desimone, S. Demoulini, R. M. Stratt, *J. Chem. Phys.* **1986**, *85*, 391.
[38] A. R. Kansal, S. Torquato, F. H. Stillinger, *Phys. Rev. E* **2002**, *66*, 041109.
[39] W. Martino, J. F. De La Mora, Y. Yoshida, G. Saito, J. Wilkes, *Green Chem.* **2006**, *8*, 390.
[40] N. Angulakshmi, K. S. Nahm, J.-M. Choi, Y. J. Hwang, A. M. Stephan, *Sci. Adv. Mater.* **2013**, *5*, 606.
[41] F. Aqra, A. Ayyad, *Appl. Surf. Sci.* **2011**, *257*, 6372.
[42] L. Ren, J. Zhuang, G. Casillas, H. Feng, Y. Liu, X. Xu, Y. Liu, J. Chen, Y. Du, L. Jiang, S. X. Dou, *Adv. Funct. Mater.* **2016**, *26*, 8111.
[43] R. Guo, X. Wang, H. Chang, W. Yu, S. Liang, W. Rao, J. Liu, *Adv. Eng. Mater.* **2018**, *20*, 1800054.
[44] U. Daalkhaijav, O. D. Yirmibesoglu, S. Walker, Y. Mengüç, *Adv. Mater. Technol.* **2018**, *3*, 1700351.
[45] H. Wang, Y. Yao, Z. He, W. Rao, L. Hu, S. Chen, J. Lin, J. Gao, P. Zhang, X. Sun, X. Wang, Y. Cui, Q. Wang, S. Dong, G. Chen, J. Liu, *Adv. Mater.* **2019**, *31*, 1901337.
[46] C. Pan, E. J. Markvicka, M. H. Malakooti, J. Yan, L. Hu, K. Matyjaszewski, C. Majidi, *Adv. Mater.* **2019**, *31*, 1900663.
[47] F. Xu, Y. Zhu, *Adv. Mater.* **2012**, *24*, 5117.
[48] M. Shin, J. H. Song, G.-H. Lim, B. Lim, J.-J. Park, U. Jeong, *Adv. Mater.* **2014**, *26*, 3706.
[49] T.-G. La, S. Qiu, D. K. Scott, R. Bakhtiari, J. W. P. Kuziek, K. E. Mathewson, J. Rieger, H.-J. Chung, *Adv. Healthcare Mater.* **2018**, *7*, 1801033.
[50] K.-Y. Chun, Y. Oh, J. Rho, J.-H. Ahn, Y.-J. Kim, H. R. Choi, S. Baik, *Nat. Nanotechnol.* **2010**, *5*, 853.
[51] B. Wang, A. Facchetti, *Adv. Mater.* **2019**, *31*, 1901408.
[52] R. W. Style, R. Boltyanskiy, B. Allen, K. E. Jensen, H. P. Foote, J. S. Wettlaufer, E. R. Dufresne, *Nat. Phys.* **2015**, *11*, 82.
[53] M. D. Bartlett, A. Fassler, N. Kazem, E. J. Markvicka, P. Mandal, C. Majidi, *Adv. Mater.* **2016**, *28*, 3726.
[54] P. S. Owuor, S. Hiremath, A. C. Chipara, R. Vajtai, J. Lou, D. R. Mahapatra, C. S. Tiwary, P. M. Ajayan, *Adv. Mater. Interfaces* **2017**, *4*, 1700240.
[55] S. Yao, Y. Zhu, *Adv. Mater.* **2015**, *27*, 1480.
[56] H. Tokuda, K. Hayamizu, K. Ishii, M. A. B. H. Susan, M. Watanabe, *J. Phys. Chem. B* **2005**, *109*, 6103.
[57] T. Takigawa, Y. Morino, K. Urayama, T. Masuda, *Polym. Gels Networks* **1996**, *4*, 1.
[58] P. H. Mott, C. M. Roland, *Phys. Rev. B* **2009**, *80*, 132104.